Terahertz birefringence and attenuation properties of wood and paper

Matthew Reid and R. Fedosejevs

The far-infrared properties of spruce wood are examined with a terahertz time-domain spectrometer. The solid wood is shown to exhibit both birefringence and diattenuation. The birefringence properties are sufficient for construction of a quarter-wave plate operating at 0.36 THz, and a half-wave plate operating at 0.71 THz. The origin of the birefringence is attributed to preferential fiber orientation within the wood. Similar birefringence is observed in lens paper in which the fibers are preferentially oriented in one direction.

OCIS codes: 230.5440, 160.4890, 160.4760.

1. Introduction

Many materials are transparent in the far infrared, making it an interesting diagnostic wavelength range for material inspection. The fact that far-infrared radiation, at the levels typically present in a terahertz time-domain spectrometer, poses no significant health hazard[1] makes it attractive for many application areas such as in imaging[2] and security.[3,4]

It was recognized early on that there may be applications in the wood industry for pulsed terahertz radiation.[5,6] This is so primarily because pulsed terahertz radiation offers access to a frequency range of transparency in wood. Koch *et. al.*[5] demonstrated that transmission imaging of wood can be performed with a resolution sufficient to allow annular rings to be distinguished by a terahertz time-domain spectrometer. However, there has been little work in this area since these early investigations.

In this paper the far-infrared properties of common spruce wood are studied in detail, and it is demonstrated that the wood exhibits both diattenuation and birefringence. We demonstrate these properties by constructing a wave plate from wood and also demonstrate the potential for fiber-orientation analysis with pulsed terahertz radiation.

Fiber orientation analysis has traditionally relied on methods involving optical scattering measurements,[7] x-ray diffraction measurements,[8,9] and the use of fiber dyes.[10] The electromagnetic methods for the determination of fiber orientation rely on the structure of the cellulose that makes up the fiber.[7–10]

In the present paper we present an alternative approach to measuring fiber orientation by using far-infrared radiation and the polarizing properties of the fibers. This method has the advantage that it can be operated in a transmission mode for samples as much as 1 cm thick, which optical techniques cannot do. Moreover, it also has the advantages that x rays are not required and that the radiation used is nonionizing and safe.[1]

2. Experiment

The experimental setup used is shown in Fig. 1 and is similar to that reported previously.[11] A semilarge-aperture photoconductive switch[12] is used as a source of terahertz radiation. The switch is formed from silver paint upon a Si–GaAs substrate with a minimum separation of 470 μm and biased with a 250 V peak, 40 kHz sine wave. The switch is driven with 300 mW of optical power from an 80 MHz, 100 fs Ti:sapphire oscillator. The optical beam is split into pump and probe beams. The pump is lightly focused on the photoconductive switch, and the emitted terahertz radiation, which is horizontally polarized, is imaged onto a 1 mm thick (110) oriented ZnTe crystal that is used to detect the radiation by means of the linear electro-optic effect[13] with four $f/2$, 2 in. (5.08 cm) diameter, 90° off-axis parabolic mirrors. The four mirrors form

When this research was performed, the authors were with the Department of Electrical and Computer Engineering, University of Alberta, Edmonton, Alberta, Canada. M. Reid (reid@ece.ualberta.ca) is now with the Department of Physics, University of Northern British Columbia, Prince George, B.C., Canada.

Received 24 May 2005; accepted 16 September 2005.
0003-6935/06/122766-07$15.00/0

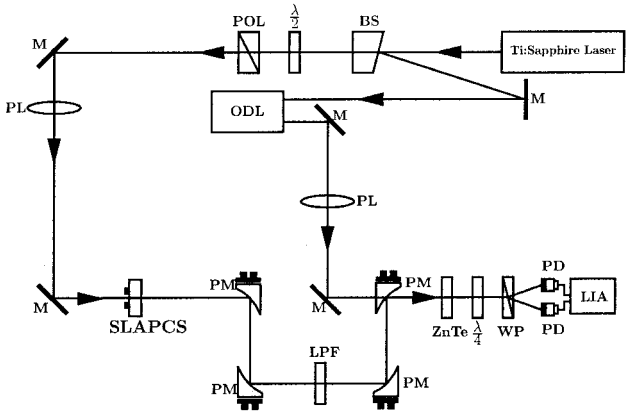

Fig. 1. Schematic diagram of the setup: BS, beam splitter; λ/2, half-wave plate; POL, polarizer; M's, mirrors; ODL, optical delay line; PLs, positive lenses; PMs, parabolic mirrors; LPF, low-pass filter blocking the optical leakage and passing the far-infrared radiation; λ/4, quarter-wave plate; WP, Wollaston prism; PDs, are photodiodes; LIA, lock-in amplifier; SLAPCS, semi-large aperture photoconductive switch.

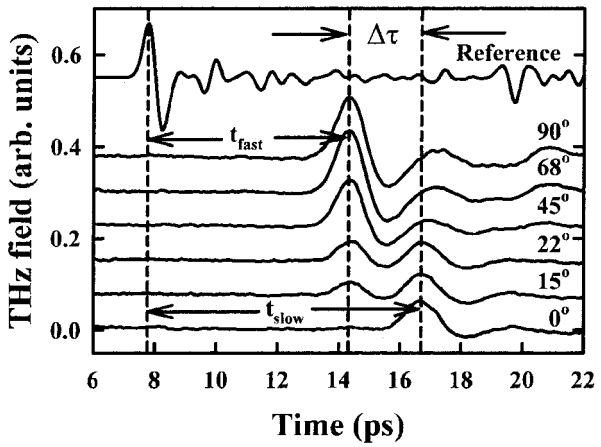

Fig. 2. Reference and transmitted terahertz time-domain waveforms transmitted through an 8.3 mm piece of spruce wood measured with the terahertz polarization making an angle θ with respect to the visible grain direction. Each scan is labeled by the corresponding value of θ used in the measurement, and the scans are offset for clarity. t_{fast} and t_{slow}, time delay for propagation with terahertz polarization perpendicular and parallel to the visible grain, leading to fast and slow axes, respectively. Δτ, time difference between terahertz propagation polarized parallel and perpendicular to the grain.

an intermediate focal plane in which the samples are placed for the studies that follow.

Polarization-sensitive measurements are made for which the ZnTe crystal is used as a polarization analyzer for the terahertz radiation.[13] The probe beam is linearly horizontally polarized, and the [001] axis of the ZnTe crystal is oriented to detect either vertically or horizontally polarized terahertz radiation at the detector.

Two samples of solid spruce wood, with thicknesses of 8.3 and 3.025 mm, were studied. The samples were purchased from a hardware store, cut to the desired size, and given a smooth finish. The samples were exposed to air and were therefore subjected to ambient humidity. The lens paper investigated in this report was standard lens paper purchased from Fisher Scientific.

3. Birefringence of Spruce

Birefringence is an interesting phenomenon in single-cycle radiation when it is viewed directly on a short time scale with pulsed radiation in the time domain. We observed the birefringence of an 8.3 mm thick piece of solid spruce wood directly in the time domain by inserting the sample into the focal plane of the parabolic mirror system at the position of the low-pass filter in Fig. 1. The measured transmission of the terahertz radiation is shown in Fig. 2.

We examined the time-domain waveforms of transmitted terahertz radiation as functions of the orientation of the grain with respect to the terahertz polarization by rotating the wood sample. The angular dependence of the transmitted terahertz field is shown in Fig. 2 with the detection set to detect horizontally polarized transmitted terahertz radiation.

If the birefringent material is made sufficiently long, and the pulse width of the electromagnetic radiation sufficiently short, then the birefringence will introduce a phase shift between orthogonal polarization components, and a corresponding propagation delay in the time domain. Specifically, if the phase difference corresponds to a time scale longer than the pulse width of the radiation, two orthogonally polarized pulses of electromagnetic radiation will result, the magnitude of which will depend on the orientation of the input polarization and the birefringent axes. When the angle between the input terahertz polarization and the visible grain is approximately 22°, as shown in Fig. 2, the output radiation comprises two pulses, roughly equal in amplitude and separated by approximately 2 ps in time with orthogonal polarization. The fact that the pulses have roughly equal amplitudes at an angle different from 45° is a consequence of the diattenuation that is present within the wood and is discussed later in this paper.

Based on the observed time delay between pulses of terahertz radiation propagating parallel and perpendicular to the visible grain, an estimate of the frequency averaged birefringence can be obtained directly from the time-domain data of Fig. 2. Assuming that the birefringence is frequency independent, then the average birefringence, Δn, over the bandwidth of the transmitted terahertz pulse is related to the time delay between propagation with polarization parallel and perpendicular to the grain, Δτ, by

$$\Delta n = c\Delta\tau/L, \tag{1}$$

where c is the speed of light in vacuum and L is the thickness of the wood.

We estimate $\Delta\tau = 2.2$ ps from Fig. 2 and, using $L = 8.3$ mm, obtain the frequency-averaged birefringence given by Eq. (1), $\Delta n = 0.08 \pm 0.01$.

As the terahertz radiation is pulsed and composed of a broad frequency spectrum, a more precise way to analyze the birefringence is to examine the index of refraction, which can be obtained from the transmitted spectrum. In fact, as the detection is coherent, we can extract the frequency-resolved complex index of refraction directly from the measured data. To do this, we use the thick sample approximation of Duvillaret *et. al.*,[14] truncating the time-domain spectrum before multiple reflections occur, and write the ratio of the measured transmission spectrum to the reference spectrum as

$$\frac{\mathbf{E}_{\text{wood}}(\nu)}{\mathbf{E}_{\text{ref}}(\nu)} = \hat{t}_{\text{AW}}\hat{t}_{\text{WA}} \exp\left[-\frac{i2\pi\nu L}{c}(\hat{n}_W - \hat{n}_A)\right], \quad (2)$$

where $\mathbf{E}_{\text{wood}}$ and $\mathbf{E}_{\text{ref}}$ are the measured terahertz fields in the frequency domain with and without wood in the beam paths, respectively, ν is the frequency, c is the speed of light in vacuum, L is the length of the wood sample, and $\hat{t}_{\text{WA}}$ and $\hat{t}_{\text{AW}}$ are the Fresnel transmission coefficients of wood-to-air and air-to-wood interfaces, respectively. The Fresnel transmission coefficients are given by

$$\hat{t}_{ij} = \frac{2\hat{n}_i}{\hat{n}_i + \hat{n}_j} \quad (3)$$

for normal incidence.[15] Writing the ratio of Eq. (2) in Euler form; $R\exp(i\theta)$, we may make use of the measured data to extract complex index $\hat{n}_W$. We take $\hat{n}_A = 1$ and

$$\hat{n}_W = n_W - ik_W, \quad (4)$$

with the approximation in the Fresnel coefficients that $k \ll n$, to obtain

$$\begin{aligned} R\exp(i\theta) &= \frac{\mathbf{E}_{\text{wood}}(\nu)}{\mathbf{E}_{\text{ref}}(\nu)} \\ &\approx \frac{4n_W}{(n_W+1)} \exp\left(-\frac{2\pi\nu L}{c} k_W\right) \\ &\quad \times \exp\left[-\frac{i2\pi\nu L}{c}(n_W - 1)\right]. \end{aligned} \quad (5)$$

Solving for n_W and k_W in relation (5) and using the equation $\alpha_W = 4\pi\nu k_W/c$, we obtain

$$n_W = -\frac{\theta c}{2\pi\nu L} + 1, \quad (6)$$

$$\alpha_W = -\frac{2}{L}\ln\left[R\,\frac{(n_W+1)^2}{4n_W}\right], \quad (7)$$

where α_W is the absorption coefficient.

To improve spectral resolution, we used a sample of spruce wood of 3.025 mm thickness to generate full frequency-resolved transmission spectra. A reference scan was taken, as well as transmission scans with the terahertz polarization parallel and perpendicular to the visible grain. The reference and transmission data were Fourier transformed to the frequency domain, and we used Eq. (6) to obtain the frequency-resolved index of refraction and absorption coefficient presented in Fig. 3. As can be clearly observed, the wood exhibits both birefringence and diattenuation.

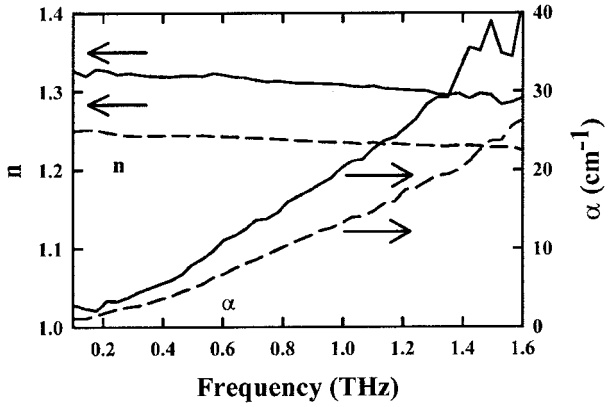

Fig. 3. Frequency-resolved index of refraction (n) and absorption coefficient (α) obtained in transmission spectroscopy of a 3.025 mm thick piece of spruce wood. Measurements were taken with the terahertz polarization parallel to the grain (solid curves) and perpendicular to the grain (dashed curves).

A frequency averaged birefringence of 0.07 ± 0.006 is measured for the frequency range 0.1–1.6 THz, in reasonable agreement with the time-domain estimate of 0.08 ± 0.01, given that different samples were used. The birefringence is also observed to be roughly frequency independent, indicating that the time-domain method of measuring birefringence should be valid.

Inasmuch as dry wood is not highly conductive, the difference in extinction for terahertz radiation propagating through the wood polarized parallel and perpendicular to the grain is possibly related to scattering. The cylindrical shape of the porous structures, which have diameters in the range 80–140 μm for spruce wood,[16] may scatter more strongly when the terahertz radiation is polarized parallel to the pores than when it is polarized perpendicular to the pore axis. For a single long, solid cylinder, the extinction coefficient is greater for polarization parallel to the cylinder axis, and the ratio of extinction coefficients ($Q^{\parallel}_{\text{ext}}/Q^{\perp}_{\text{ext}}$) grows with increasing frequency in the range of interest,[17] similar to that described in the present paper.

Given that the indices of refraction for these samples of solid wood are in the range 1.25–1.35, the measured value for $\Delta n = 0.07 \pm 0.006$ is a large birefringence. We demonstrate this large birefringence by constructing waveplates for use at far infrared frequencies.

4. Investigation of Wave Plates Constructed from Spruce

We investigated the operation of a 3.025 mm thick piece of spruce as both a quarter- and a half-wave

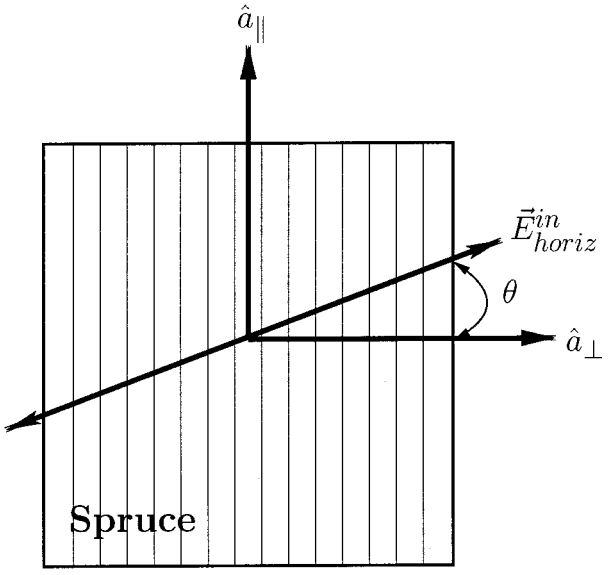

Fig. 4. Schematic diagram of the orientation of the wood with respect to analyzer axes (vertical and horizontal) for the input terahertz fields. Directions $\hat{a}_{\|}$ and $\hat{a}_{\perp}$ are parallel and perpendicular, respectively, to the wood grain.

plate for specific frequencies. First we computed what is expected for such devices when diattenuation is present. To do this we calculated the angular dependence of the vertically and horizontally polarized terahertz fields after their propagation through a 3.025 mm thick piece of spruce. Consider the geometry shown in Fig. 4.

The field at the output of the wood parallel ($E_{\|}$) and perpendicular ($E_{\perp}$) to the grain structure is given by

$$E_{\perp}^{\text{out}} = E_{\text{in}} \cos(\theta)\exp(i\Gamma_{\perp})\exp(-\tfrac{1}{2}\alpha_{\perp}d),$$

$$E_{\|}^{\text{out}} = E_{\text{in}} \sin(\theta)\exp(i\Gamma_{\|})\exp(-\tfrac{1}{2}\alpha_{\|}d), \tag{8}$$

where E_{in} is the incident electric field amplitude, θ is as defined in Fig. 4, $\Gamma_{\|}$ and $\Gamma_{\perp}$ are the phase retardances incurred along the grain and perpendicular to the grain, respectively, d is the thickness of the wood sample, and $\alpha_{\|}$ and $\alpha_{\perp}$ are the power absorption coefficients parallel and perpendicular to the grain, respectively.

In Fig. 4 the output fields along the two grain axes recombine to form horizontally and vertically polarized THz fields at the output, to which our analyzer is sensitive. The vertical and horizontal components are given by

$$E_{\text{vert}}^{\text{out}} = E_{\|}^{\text{out}} \cos(\theta) - E_{\perp}^{\text{out}} \sin(\theta),$$

$$E_{\text{horiz}}^{\text{out}} = E_{\perp}^{\text{out}} \cos(\theta) + E_{\|}^{\text{out}} \sin(\theta). \tag{9}$$

Using Eqs. (8) in Eqs. (9), we obtain the angular dependence of the magnitude of the horizontal and vertical components of the output field along the analyzer axes:

$$\begin{aligned}\left|E_{\text{vert}}^{\text{out}}\right| &= |E_{\text{in}}|\exp(-\tfrac{1}{2}\alpha_{\|}d) \\ &\quad \times |\sin(\theta)\cos(\theta)| \\ &\quad \times |1 - \exp(i\Delta\Gamma)\exp(-\Delta\alpha d)|,\end{aligned}$$

$$\begin{aligned}\left|E_{\text{horiz}}^{\text{out}}\right| &= |E_{\text{in}}|\exp(-\tfrac{1}{2}\alpha_{\|}d) \\ &\quad \times \left|\cos^2(\theta)\exp(-\Delta\alpha d)\exp(i\Delta\Gamma)\right. \\ &\quad \left. + \sin^2(\theta)\right|,\end{aligned} \tag{10}$$

where $\Delta\alpha = \frac{1}{2}(\alpha_{\perp} - \alpha_{\|})$ and $\Delta\Gamma = \Gamma_{\perp} - \Gamma_{\|}$ are the differences in absorption and induced phase for propagation along the grain and perpendicular to the grain, respectively.

Finally, taking Eqs. (10) with $\Delta\Gamma = \pi/2$ and $\Delta\Gamma = \pi$, the expressions for the terahertz field magnitudes as a function of the angular orientation of the wood for quarter- and half-wave plate behavior are obtained:

$$\begin{aligned}E_{\text{vert}}^{\text{out, QWP}} &= E_{\text{in}}\exp(-\tfrac{1}{2}\alpha_{\|}d)|\sin(\theta)\cos(\theta)| \\ &\quad \times [1 + \exp(-2\Delta\alpha)]^{1/2},\end{aligned}$$

$$\begin{aligned}E_{\text{vert}}^{\text{out, HWP}} &= E_{\text{in}}\exp(-\tfrac{1}{2}\alpha_{\|}d)|\sin(\theta)\cos(\theta)| \\ &\quad \times [1 + \exp(-\Delta\alpha d)],\end{aligned}$$

$$\begin{aligned}E_{\text{horiz}}^{\text{out, QWP}} &= E_{\text{in}}\exp(-\tfrac{1}{2}\alpha_{\|}d) \\ &\quad \times \left[\sin^4(\theta) + \cos^4(\theta)\right. \\ &\quad \left. \times \exp(-2\Delta\alpha d)\right]^{1/2},\end{aligned}$$

$$\begin{aligned}E_{\text{horiz}}^{\text{out, HWP}} &= E_{\text{in}}\exp(-\tfrac{1}{2}\alpha_{\|}d) \\ &\quad \times \left(\left\{\sin^2(\theta)[1 + \exp(-\Delta\alpha d)]\right.\right. \\ &\quad \left.\left. - \exp(-\Delta\alpha d)\right\}^2\right)^{1/2}.\end{aligned} \tag{11}$$

Note that only specific frequencies will meet the criteria for $\Delta\Gamma = \pi/2$ and $\Delta\Gamma = \pi$. We estimate the matching wavelength using the desired phase retardance and birefringence (Δn) as

$$\lambda_{\text{match}} = \frac{2\pi L}{\Delta\Gamma}\,\Delta n, \tag{12}$$

where λ_{match} is the matching wavelength, Δn is the birefringence, and $\Delta\Gamma$ is the desired phase retardance. From Fig. 3 we have an approximately frequency-independent birefringence of $\Delta n = 0.07 \pm 0.006$, which gives matching wavelengths of 847 μm (or 0.35 THz) and 424 μm (or 0.71 THz) for quarter-wave ($\Delta\Gamma = \pi/2$) and half-wave ($\Delta\Gamma = \pi$) phase retardance, respectively, for a 3.025 mm thick piece of spruce.

Taking terahertz time-domain scans as a function of the angle θ in Fig. 4, and Fourier transforming to the frequency domain, we obtain a set of frequency spectra. The amplitudes in specific frequency bins,

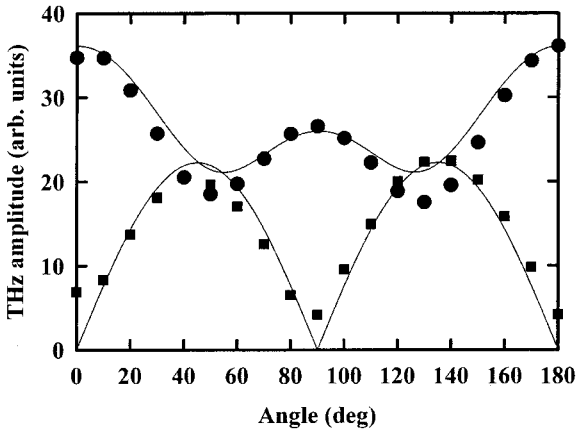

Fig. 5. Measured THz transmission for the 365 GHz frequency bin data as a function of wood orientation. The data for vertically (squares) and horizontally (circles) polarized terahertz fields are shown for transmission through 3.025 mm thick spruce, along with the expected angular dependence for behavior as a quarter-wave plate [Eqs. (11)]. The angle is defined as the angle that the grain direction makes with the vertical axis.

with a width of 40 GHz, are computed to form an angularly resolved measurement for each frequency bin. Both horizontally polarized and vertically polarized transmitted terahertz fields are measured in this way. The result is plotted in Fig. 5 for a frequency bin centered at 0.356 THz. The solid curves show data expected for the birefringence as given by Eqs. (11).

A similar result is obtained for operation of the 3.025 mm thick spruce wood as a half-wave plate. In this case the best fit to the data is for the 0.71 THz frequency bin, as expected based on the matching wavelength calculated above. The angularly resolved *s*- and *p*-polarized transmitted fields at 0.71 THz are plotted in Fig. 6, together with the output predicted when Eqs. (11) are used.

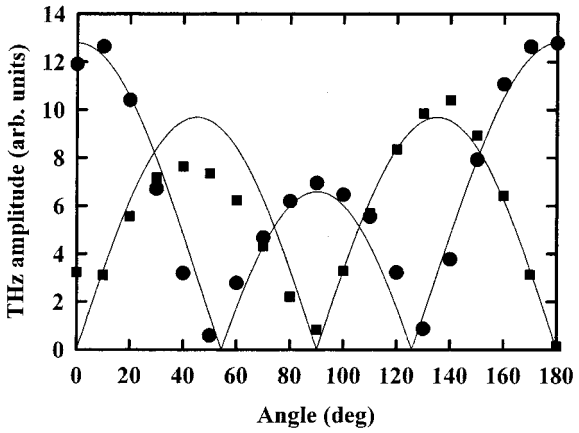

Fig. 6. THz transmission for the 711 GHz frequency bin data as a function of wood orientation. The data for vertically (squares) and horizontally (circles) polarized terahertz fields are shown for transmission through 3.025 mm thick spruce, along with the expected angular dependence for behavior as a half-wave plate [Eq. (11)]. The angle is defined as the angle that the grain direction makes with the vertical axis.

These results clearly demonstrate the behavior of spruce as a wave plate for frequencies in the far infrared: Whereas it is likely not a practical device owing to significant attenuation within the wood, the possibility of constructing birefringent elements from wood is clearly demonstrated.

5. Fiber-Orientation Analysis by Terahertz Time-Domain Spectroscopy

Paper products are derivatives of wood and therefore contain wood fiber. The fiber of the wood is what leads to the birefringence that was demonstrated above. Therefore, depending on whether there is a preferential orientation of the fibers within a paper product, one might expect paper also to exhibit birefringence. Lens paper is a typical example of such a product, and it is easily verified that lens paper has a preferential fiber orientation, which one can most easily observe by tearing the paper. One will find that the paper preferentially tears along one fixed direction, while it is difficult to tear the paper in any other direction.

The birefringence associated with this fiber orientation is easily verified. A collection of 27 pieces of identically oriented lens paper was put in the terahertz spectrometer setup. It was immediately observed that the position of the peak of the terahertz pulse in the time domain (see Fig. 7) changed as a function of the orientation of the lens paper with respect to the polarization of the terahertz beam. This is the time-domain manifestation of birefringence outlined above.

In fact, the orientation of the fibers with respect to the polarization of the terahertz beam is easily mapped out by use of the change in time delay as a function of the orientation of the lens paper. Consider that the indices of refraction are $n_\perp$ and $n_\parallel$ when the polarization of the terahertz radiation is perpendicular and parallel, respectively, to the preferential fiber orientation; and the 27 pieces of lens paper form a sample of thickness d_{lens}. Then time delay $\Delta\tau$ as a function of the orientation of the lens paper with respect to the terahertz polarization is given by

$$\Delta\tau = \frac{d_{\text{lens}}}{c}\,[n_\perp \cos(\theta) + n_\parallel \sin(\theta)], \tag{13}$$

where c is the speed of light in vacuum, θ is the angle that the linear polarization of the terahertz radiation makes with the vector perpendicular to the fiber orientation, and the quantity in brackets is the effective index of refraction for propagation through the lens paper at normal incidence for this polarization state.

This time delay is most easily measured on a portion of the terahertz time-domain waveform that is rapidly changing in time. Therefore we choose a rapidly varying linear portion of the terahertz time-domain waveform as the operating point, as shown in Fig. 7.

Once the optical delay-line is fixed at the operating point shown in Fig. 7, the signal on the lock-in amplifier is zeroed. The resultant change in signal as the

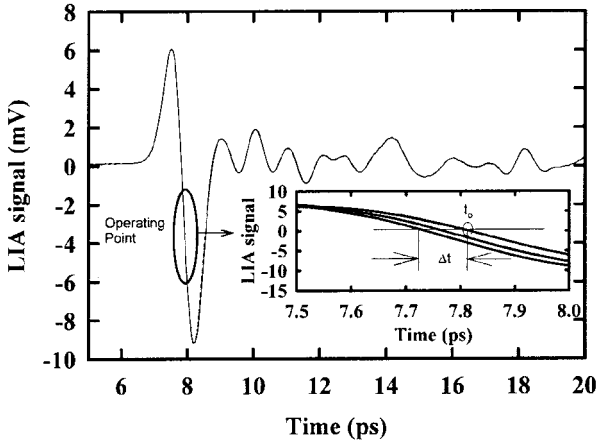

Fig. 7. Operating point for mapping the time delay of terahertz radiation to birefringence data. The figure shows a typical terahertz time-domain waveform, and the orientation of the operating point is shown in the inset. The lock-in amplifier (LIA) signal is zeroed at the operating point, and the lens paper sample is rotated about its surface normal to map the time delay to amplitude information.

orientation of the lens paper is changed is a direct measure of $\Delta\tau$. The result is plotted in Fig. 8.

The lock-in amplifier's signal (time delay) is negative in Fig. 8 because the angle is defined as the angle that the linearly polarized terahertz beam makes with the fiber orientation. As the fiber axis is the slow axis, as the angle is rotated by 90° ($E_{\mathrm{THz}} \| n_{\perp}$) it falls along the fast axis and therefore arrives earlier, leading to negative time delays and a decrease in signal owing to the operating point chosen. Once the data are taken over an angular range of 90°, it is possible to determine the orientation of the polarization with respect to the preferential fiber alignment at an arbitrary position.

The important point for a practical application is that a full terahertz time-domain waveform is unnecessary. A simple measurement of a relative lock-in amplifier signal (time delay) is sufficient once the indices of refraction are known and the operating point is chosen.

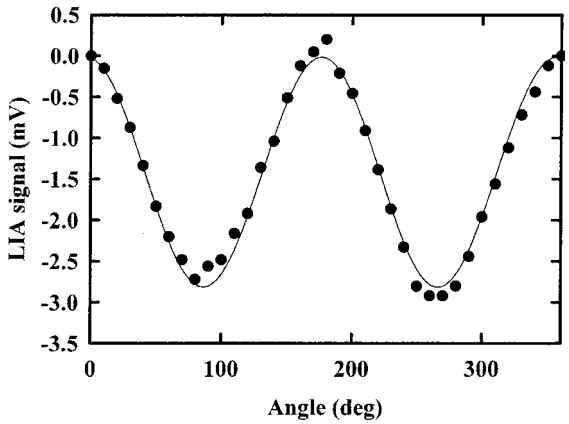

Fig. 8. Lock-in amplifier (LIA) signal as a function of orientation for transmission of terahertz radiation through 27 pieces of aligned lens paper. The lens paper oriented with its fiber alignment vertical corresponds to 0° here. The input terahertz field is polarized horizontally. The measured signal corresponds to mapping time delay to birefringence (see text for details).

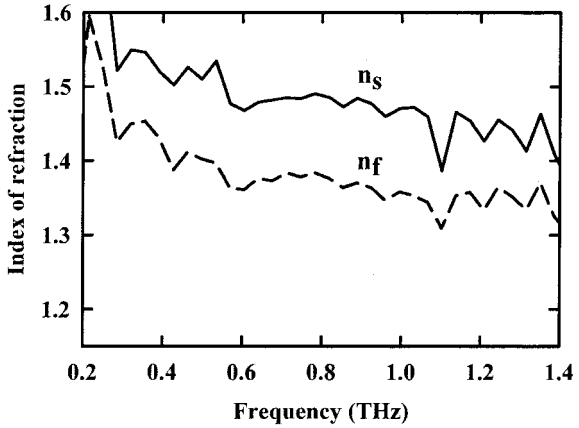

Fig. 9. Index of refraction of a 21 μm thick piece of lens paper obtained with terahertz polarization perpendicular (long-dashed curve) and parallel (solid curve) to the fiber orientation. n_f, n_s, fast and slow axes, respectively.

Another important point for practical applications is that the time required for obtaining data over a 90° span is essentially limited by the lock-in time constant. In this case a lock-in amplifier time constant of 100 ms was used, such that a 90° scan could take a fraction of a second.

Finally, a single piece of lens paper, 21 μm thick, was measured by use of a terahertz time-domain waveform acquired in 3 s, limited by the speed of the optical delay line, for each polarization orientation. A reference scan is taken; then, a transmission scan with the terahertz polarization parallel and perpendicular to the grain. The complete frequency-resolved measurement of the indices of refraction is computed, and the data are presented in Fig. 9.

The frequency-resolved index measurements of the single piece of lens paper demonstrate that birefringence is quite large in the lens paper, with a frequency-averaged value of $\Delta n = 0.10 \pm 0.03$ in the frequency range 0.2–1.4 THz. The data are fairly noisy as a consequence of the short time scan for the transmission measurements and of the fact that the reference and transmitted signals are only slightly different.

As a final remark, it should be pointed out that other fibrous materials are expected to produce effects similar to those observed in the present paper. This indicates that there is potential for engineered fibrous structures that could, for example, be made to reduce diattenuation, which was observed to be large in solid wood. Such structures may provide a unique opportunity for studying and constructing polarization-affecting materials.

6. Conclusions

It was demonstrated that solid spruce wood is birefringent, with a birefringence of 0.07 ± 0.006, which

is approximately frequency independent in the range 0.1–1.6 THz. The extinction coefficient was shown to depend on the terahertz polarization and therefore exhibit diattenuation. The birefringence was investigated in detail for quarter- and half-wave plate configurations centered at 0.36 and 0.72 THz, respectively, showing more complex behavior owing to the diattenuation. The fiber alignment in standard laboratory lens paper was also measured by use of THz radiation and served to demonstrate the possibility of using pulsed terahertz radiation for fiber orientation analysis of single sheets of lens tissue.

This work was supported by MPB Technologies, Inc., and the Natural Sciences and Engineering Research Council (Canada). (M. Reid) acknowledges partial financial support provided by Informatics Circle of Research Excellence.

References and Notes

1. G. C. Walker, E. Berry, N. N. Zinov'ev, A. J. Fitzgerald, R. E. Miles, M. Chamberlain, and M. A. Smith, "Teraherz imaging and international safety guidelines," in *Medical Imaging 2002: Physics of Medical Imaging*, L. E. Antonuk and M. J. Yaffe, eds., Proc. SPIE **4682,** 683–690 (2002).
2. D. M. Mittleman, M. Gupta, R. Neelamani, R. G. Baraniuk, J. V. Rudd, and M. Koch, "Recent advances in terahertz imaging," Appl. Phys. B **68,** 1085–1094 (1999).
3. M. C. Kemp, P. F. Taday, B. E. Cole, J. A. Cluff, A. J. Fitzgerald, and W. R. Tribe, "Security applications of terahertz imaging," in *Terahertz for Military and Security Applications,* R. J. Hwu and D. L. Woolard, eds., Proc. SPIE **5070,** 44–52 (2003).
4. W. R. Tribe, D. A. Newnham, P. F. Taday, and M. C. Kemp, "Hidden object detection: security applications of terahertz technology," in *Terahertz and Gigahertz Electronics and Photonics III,* R. J. Hwu, ed., Proc. SPIE **5354,** 168–176 (2004).
5. M. Koch, S. Hunsche, P. Schaucher, M. C. Nuss, J. Feldmann, and J. Fromm, "THz-imaging: a new method for density mapping of wood," Wood Sci. Technol. **32,** 421–427 (1998).
6. S. Hunsche and M. C. Nuss, "Terahertz T-ray tomography," in *Millimeter and Submillimeter Waves IV*, M. N. Afsar, ed., Proc. SPIE **3465,** 426–433 (1998).
7. Y. W. Lim, A. Sarko, and R. H. Marchessault, "Light scattering by cellulose. II. Oriented condensed paper," TAPPI J. **53,** 2314–2319 (1970).
8. P. H. Friedlander, "The measurement of fibre orientation in newsprint with respect to the machine direction by x-ray diffraction," Pulp Paper Mag. Canada (January 1958), pp. 102–103.
9. H. Ruck and H. Krässig, "The determination of fiber orientation in paper," Pulp Paper Mag. Canada (June 1958), pp. 183–190 (1958).
10. C. M. Crosby, A. R. K. Eusufazi, R. E. Mark, R. W. Perkins, J. S. Chang, and N. V. Uplekar, "A digitizing system for quantitative measurement of structural parameters in paper," TAPPI J. **64,** 103–106 (1981).
11. M. Reid and R. Fedosejevs, "Quantitative comparison of THz emission from (100) InAs surfaces and GaAs large-aperture photoconductive switch at high fluences," Appl. Opt. **44,** 149–153 (2004).
12. G. Zhao, R. N. Schouten, N. van der Valk, W. T. Wenckebach, and P. C. M. Planken, "Design and performance of THz emission and detection setup based on a semi-insulating GaAs emitter," Rev. Sci. Instrum. **73,** 1715–1719 (2002).
13. P. C. M. Planken, H.-K. Nienhuys, H. J. Bakker, and T. Wenckebach, "Measurement and calculation of the orientation dependence of terahertz pulse detection in ZnTe," J. Opt. Soc. Am. B **18,** 313–317 (2001).
14. L. Duvillaret, F. Garet, and J.-L. Coutaz, "A reliable method for extraction of material parameters in terahetz time-domain spectroscopy," IEEE J. Sel. Top. Quantum Electron. **2,** 739–746 (1996).
15. J. D. Jackson, *Classical Electrodynamics,* 3rd ed. (Wiley, 1999).
16. A. J. Stamm, *Wood and Cellulose Science,* 1st ed. (Ronald Press, 1964).
17. For a long solid cylinder, with an index of refraction of 1.5, numerical calculations are shown in Fig. 67 of Ref. 18 for values of $0.1 < p < 1$, corresponding to a frequency range of 0.1–1 THz for a cylinder radius of 50 μm.
18. H. C. van de Hulst, *Light Scattering by Small Particles,* 1st ed. (Dover, 1981).